

Bioinspiration & Biomimetics



PAPER

A laser-engraved glass duplicating the structure, mechanics and performance of natural nacre

Seyed Mohammad Mirkhalaf Valashani and Francois Barthelat

Department of Mechanical Engineering, McGill University, 817 Sherbrooke Street West, Montreal, Quebec, H3A 2K6, Canada

E-mail: francois.barthelat@mcgill.ca

Keywords: bio-inspiration, nacre-like materials, composites, toughened glasses

RECEIVED
24 November 2014

REVISED
23 January 2015

ACCEPTED FOR PUBLICATION
28 January 2015

PUBLISHED
30 March 2015

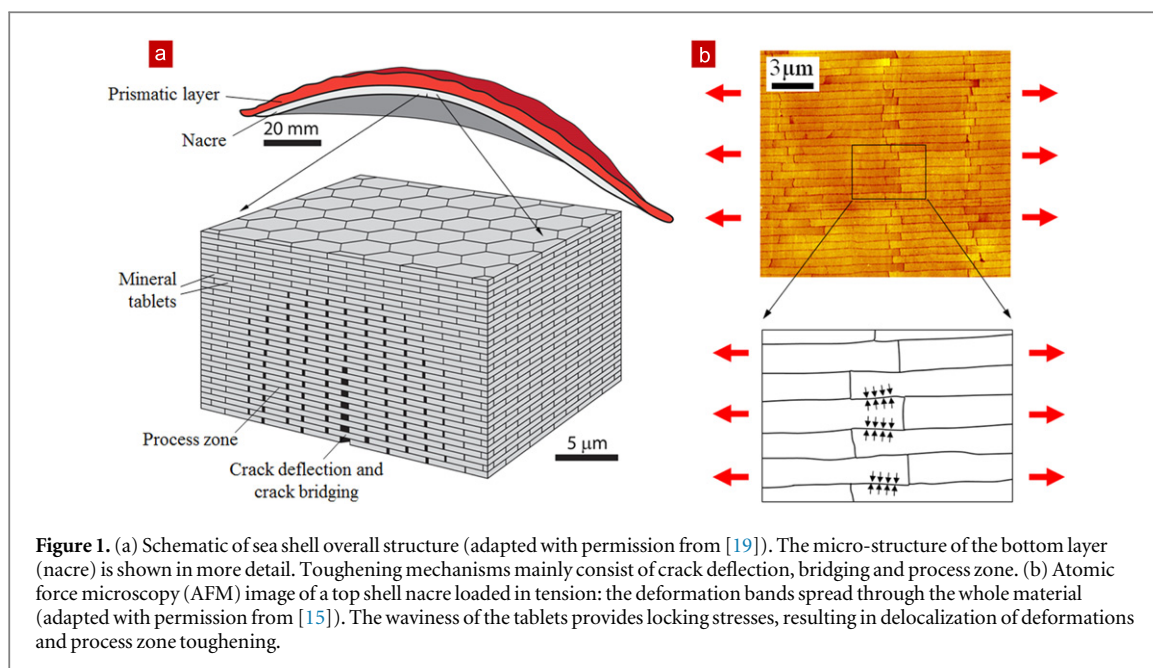
Abstract

Highly mineralized biological materials such as nacre (mother of pearl), tooth enamel or conch shell boast unique and attractive combinations of stiffness, strength and toughness. The structures of these biological materials and their associated mechanisms are now inspiring new types of advanced structural materials. However, despite significant efforts, no bottom up fabrication method could so far match biological materials in terms of microstructural organization and mechanical performance. Here we present a new 'top down' strategy to tackling this fabrication problem, which consists in carving weak interfaces within a brittle material using a laser engraving technique. We demonstrate the method by fabricating and testing borosilicate glasses containing nacre-like microstructures infiltrated with polyurethane. When deformed, these materials properly duplicate the mechanisms of natural nacre: combination of controlled sliding of the tablets, accompanied with geometric hardening, strain hardening and strain rate hardening. The nacre-like glass is composed of 93 volume % (vol%) glass, yet 700 times tougher and breaks at strains as high as 20%.

1. Introduction

Despite significant progress, the range of applications of ceramics and glasses is still hindered by their inherent brittleness. Amongst the many toughening strategies developed in the past, the incorporation of weak interfaces has been one of the most efficient [1]. Weak interfaces can intercept and deflect incoming cracks, and when properly arranged they can channel cracks into configurations where propagation is more difficult. Multilayered ceramics and glasses rely on this principle and display toughness values several orders of magnitude higher than those of their monolithic forms. In these engineering materials the geometry of the interfaces is relatively simple and as effective as they are, their architecture pales compared to the three-dimensional networks of weak interfaces found in mineralized biological tissues such as bone, teeth or mollusk shells. These natural materials are stiff and hard because of their high mineral contents, yet they are also tough because the weak interfaces they contain can intercept propagating cracks and trigger unusual and powerful toughening mechanisms [2]. For example, complex three-dimensional cross-ply stabilize

cracks by crack bridging in tooth enamel or conch shell [3, 4], Bouligand structures twist cracks to reduce driving force in the cuticle of arthropods [5], brick and mortar structures deflect cracks and lead to large deformation and toughening mechanisms in bone and nacre [6–9]. These sophisticated mechanisms are possible because propagating cracks are deflected and channeled along weak interfaces within the materials. In addition, these interfaces are filled with proteins and/or polysaccharides with unusual mechanisms such as sacrificial bonds and molecular unfolding [10] or controlled breaking and reforming of hydrogen bonds [11], which generate cohesion and energy dissipation over large crack openings (in contrast with the brittle interfaces used in engineering layered ceramics). Duplicating the complex structures and mechanisms of high-performance biological materials in synthetic materials has been an ongoing challenge for two decades. Amongst natural materials, nacre from mollusk shells has become a model for biomimetic ceramics and composites, particularly due to its unprecedented toughness amplification and relatively simple brick and mortar microstructure [12, 13]. Nacre forms the inner layer of mollusk shells. It is



composed of 95 wt% aragonite (a crystalline form of CaCO_3) and 5 wt% biopolymers (figure 1(a)) consisting mainly of β -chitin, glycine and alanine-rich proteins. The dominating structural characteristic in nacre is a brick and mortar arrangement, where each brick is a $\sim 0.5 \mu\text{m}$ thick, $5\text{--}10 \mu\text{m}$ wide aragonite polygonal tablet bonded to the adjacent tablets by 20 nm thick organic adhesives [14]. The positions of the tablets are shifted from one layer to the next so that nacre has a staggered structure (figures 1(a) and (b)) [15]. While nacre has a hierarchical structure, its large deformation capabilities and toughness are largely governed by its brick and mortar structure at the microscale. When the material undergoes tension, the tablets can slide on one another in regions of high stresses, dissipating energy and preventing crack propagation [9, 16]. If, however, a crack propagates, powerful mechanisms such as crack deflection, bridging and process zone make propagation increasingly difficult and stabilize cracks, mitigating the effect of damage [9]. These inelastic deformation mechanisms propagate over large volumes thanks to the mechanical stability of the biopolymers at the interfaces, to the geometric hardening produced by waviness of the tablets [17] and to the strain rate hardening at the interface [18].

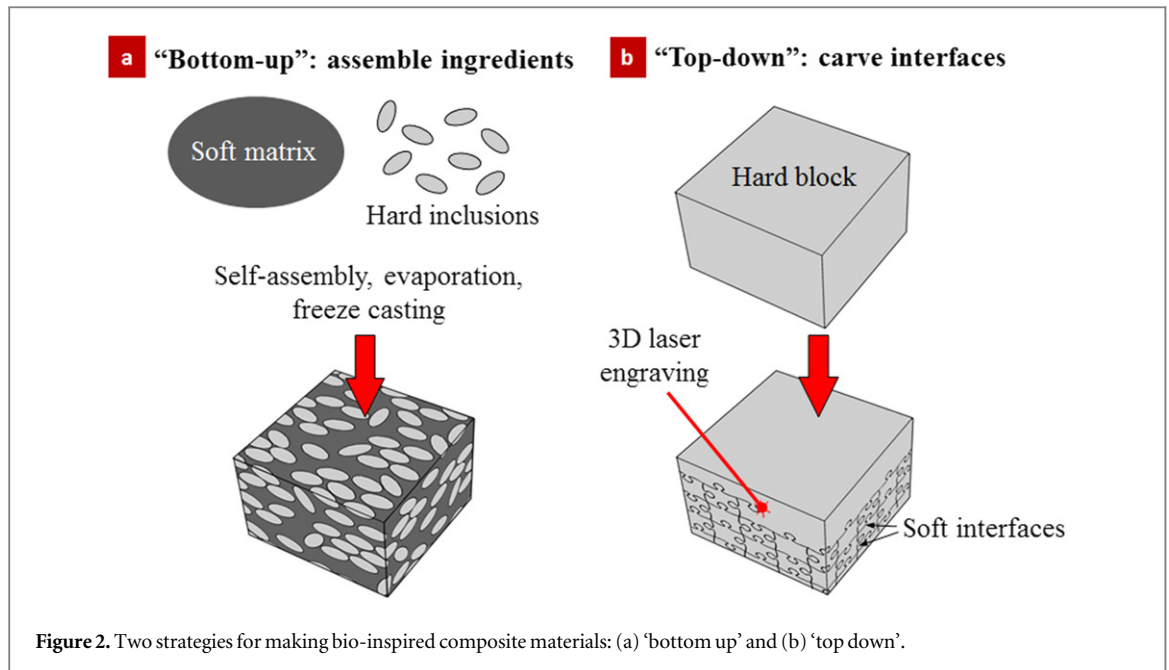
The duplication of these structures and mechanisms can provide a pathway towards new combinations of structural properties in engineering materials. Towards this goal several innovative approaches were proposed [20] including layer-by-layer assembly [21, 22], Langmuir–Blodgett film assembly [23], self-assembly [24], sedimentation [25], casting [26, 27], freeze-casting [28–30], and ink-jet deposition [31].

Several numerical and analytical studies [32] also examined the effect of different design parameters such as relative properties and arrangement of the hard and soft phases, tablet aspect ratio and waviness, mineral

concentration, flaw size within the tablets, nanoasperities, and mineral nano-pillars across the interfaces on the mechanical properties of nacre and nacre-like staggered composites [9, 17, 33–39]. Several design guidelines are concluded from these studies: (i) the overall mechanical properties of staggered composites improve by increasing the hard phase [9, 33], (ii) increasing the aspect ratio of the tablets and the overlap between them improve the properties of the material until the tablets start to break resulting in degradation of the toughness [17], (iii) with a fixed composition and aspect ratio of the tablets, the relative arrangement of the constituents has important implications on the behavior of the material [34, 39], (iv) tablets waviness results in geometrical locking which is a strong hardening mechanism preventing strain localization and improving toughness [17, 35] (v) smaller tablet size results in higher strength and toughness [36, 37], (vi) nano-asperities and mineral pillars have important effects on the stiffness, strength, and toughness of the material [38].

Despite significant theoretical and experimental advances in each of the briefly discussed studies, the duplication of the microstructure, mechanics and performance of natural nacre remains, to this day, a formidable challenge and even the best of the nacre-like materials are still far from the highly regular brick and mortar structure of natural nacre. A closer duplication of this microstructure, however, have been achieved at larger length scales which enable a better control over structures. These methods include rapid prototyping [13, 40] or direct assembly [41], and operate at scales in the order of millimeters.

A concept which permeates all these existing approaches is ‘bottom-up’ fabrication (figure 2(a)), which consists in fabricating individual building blocks and subsequently assembling them. Assembling microstructures which approach the



architecture of natural nacre still present major challenges. Here we attacked this problem from a different angle which would fall into the category of ‘top down’ fabrication. The method consists of carving networks of weak interfaces within the bulk of a hard material (ceramics or glasses). The interfaces generate microstructures which are small in size and highly controlled geometrically. Furthermore, since much of the bulk remains intact in the process of making interfaces, the method provides an easy and simple pathway towards materials with very high fractions of hard material. Similar high concentrations of the hard phase (90–99 vol%) are found in nacre or tooth, and were demonstrated to be optimal for overall mechanical performance [39]. The approach also shifts the emphasis on designing and fabricating thin interfaces within the bulk of materials (figure 2(b)) rather than designing and assembling hard building blocks. We recently illustrated this approach by engraving jigsaw-like weak interfaces within glass using a pulsed laser. Laser-generated weak interfaces could deflect and guide cracks into configuration where their propagation is more difficult, effectively making glass 200 times tougher [19]. Here, we extend the method to a nacre-like material which relies on a combination of geometric hardening, strain hardening and strain rate hardening to achieve nacre-like mechanics and performance.

2. Fabrication of a nacre-like glass

The fabrication of the architected nacre-like glass commenced by engraving thin borosilicate glass slides using three-dimensional laser engraving. The laser engraver (Model Vitrolux, Vitro Laser Solutions UG, Minden, Germany) uses a pulsed UV laser beam

(355 nm, 0.5 W cw pumped, 4 kHz repetition rate, 4–5 ns pulse duration) directed and focused at pre-defined points in space using a set of mirrors and a focusing lens (figure 3(a)). The materials were 150 μm thick rectangular (22 \times 40 mm) optical grade 263 M borosilicate glass slides (Fisher Scientific Catalog NO. 12545C, Ottawa, ON). The unfocused laser did not alter the structure of glass, and only at the focal point was the energy delivered to the material sufficient to generate defects in the form of micro-cavities and micro-cracks from thermal stresses (figure 3(b)). Thousands of individual micro-defects were generated with high spatial resolution and within minutes. Arrays of these defects formed weak interfaces capable of deflecting and guiding cracks following the principle of stamp holes. The patterns we engraved consisted of two dimensional nacre-like interfaces engraved through the thickness of the glass slides (figure 3(c)), with a laser power of 105 ± 5 mW and a spacing of 2 μm (horizontal interfaces) and 2.5 μm (vertical junctions). These parameters produced very weak interfaces through the thickness of the glass slides, in addition to ~ 75 μm deep trenches on the surface. Once these patterns were engraved, the interfaces were infiltrated with a polymeric adhesive. We experimented with different adhesives and found their mechanical behavior to be critical to the performance of the nacre-like glass. In order to obtain a nacre-like mechanical behavior, the properties of the polymers must reflect, as close as possible, the behavior of the biopolymers present at the interfaces of natural nacre: (i) strong adhesion to the tablets (ii) large deformations in shear, (iii) shear strength high enough to promote high strength of the composite, yet sufficiently low to promote tablet sliding over tablet fracture and (iv) a viscous mechanism to absorb mechanical energy and generate toughness. These

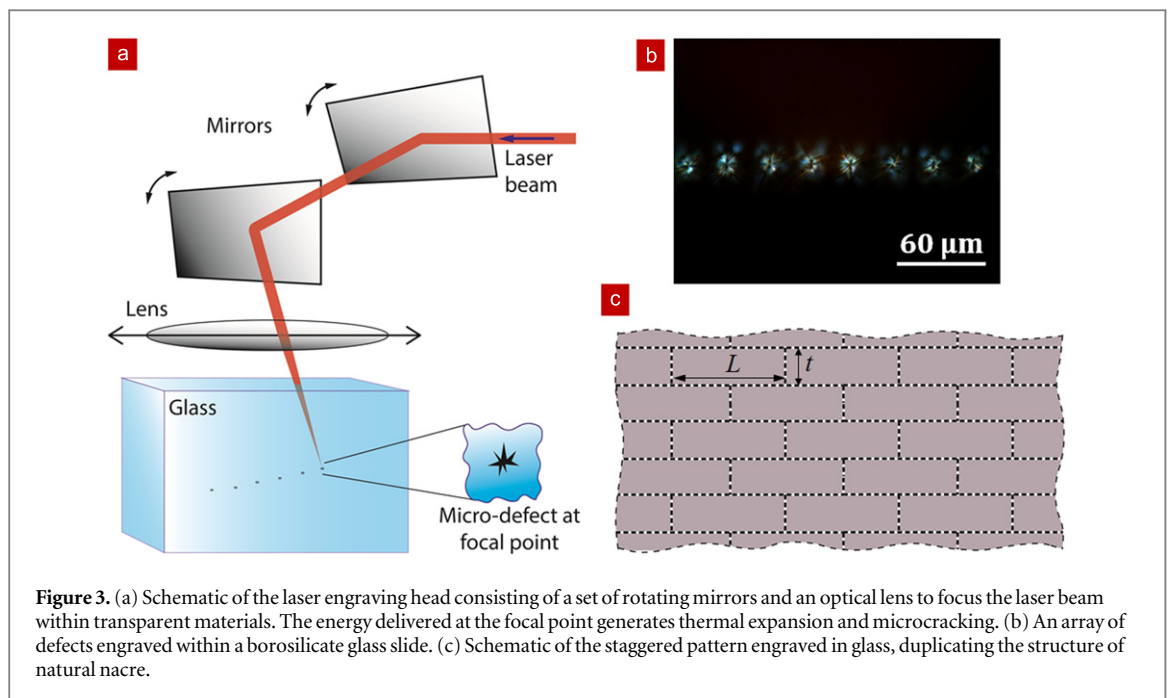


Figure 3. (a) Schematic of the laser engraving head consisting of a set of rotating mirrors and an optical lens to focus the laser beam within transparent materials. The energy delivered at the focal point generates thermal expansion and microcracking. (b) An array of defects engraved within a borosilicate glass slide. (c) Schematic of the staggered pattern engraved in glass, duplicating the structure of natural nacre.

criteria excluded cyanoacrylates which are strong but too brittle. Epoxy adhesives were more deformable but their strength was too high, resulting in fracture of the tablets. On the other end of the spectrum of properties, we found that polydimethylsiloxane was too weak and resulted in overall low material strength. We ultimately identified polyurethane (PU) (U-09FL Loctite, CT, US) as the best choice for the interfaces. This type of PU has high adhesion to glass, and it fails at large strains by formation of ligaments, in a way similar to the failure of natural proteins in nacre [10]. The PU adhesive also provided an elastomeric response with a strain stiffening mechanism at the interfaces which delayed localization, spreading the deformation through the material. Finally, the PU we selected has a low viscosity prior to curing, which enabled deep infiltration within the engraved glass. The first type of nacre-like material we fabricated had straight interfaces, with geometry characterized by two parameters: the thickness of the tablets t and their aspect ratio $\rho = \frac{L}{t}$, where L is the length of the tablets (figure 3(c)). The resulting materials were composed of 93 vol% glass and 7 vol% PU.

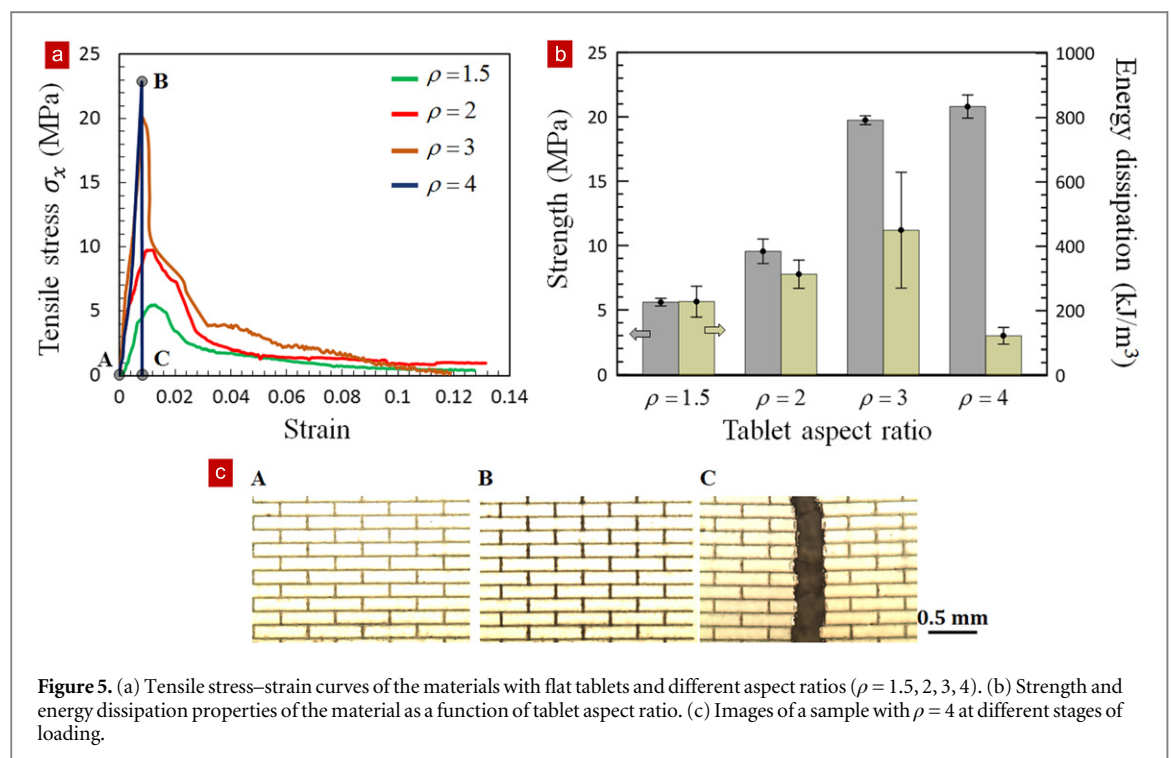
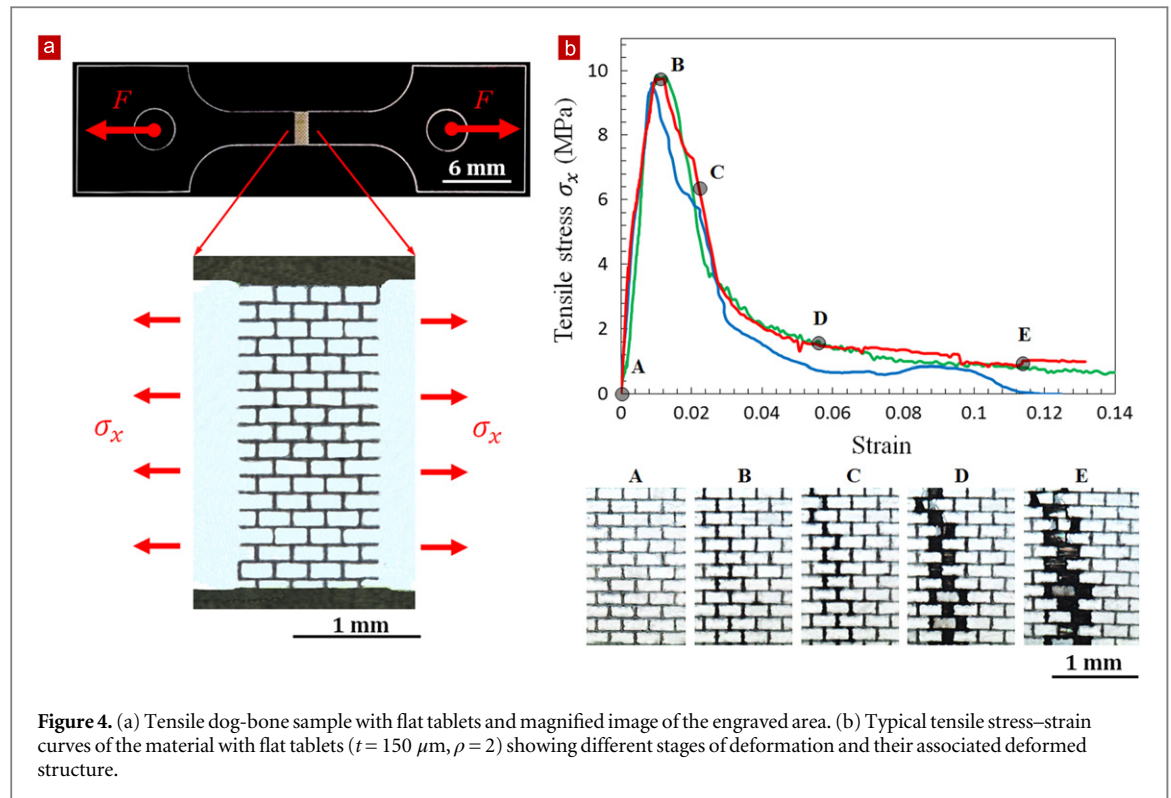
3. Tensile performance

The nacre-like pattern above was engraved into a tensile dog-bone glass sample (figure 4(a)) which contained four columns of tablets along the longitudinal direction and eighteen layers of tablets in transverse direction. After infiltration with PU, the samples were tested in tension at a displacement rate of $5 \mu\text{m s}^{-1}$ on a miniature loading machine (Ernest F Fullam, Inc., Latham, NY, USA) placed under an upright optical microscope (BX-51 M, Olympus,

Markham, Canada). *In situ* imaging of the material enabled accurate determination of the strains by Digital Image Correlation (DIC) using the commercial software VIC-2D (Correlated Solutions, SC, USA), and also enabled the monitoring of the deformation and failure modes.

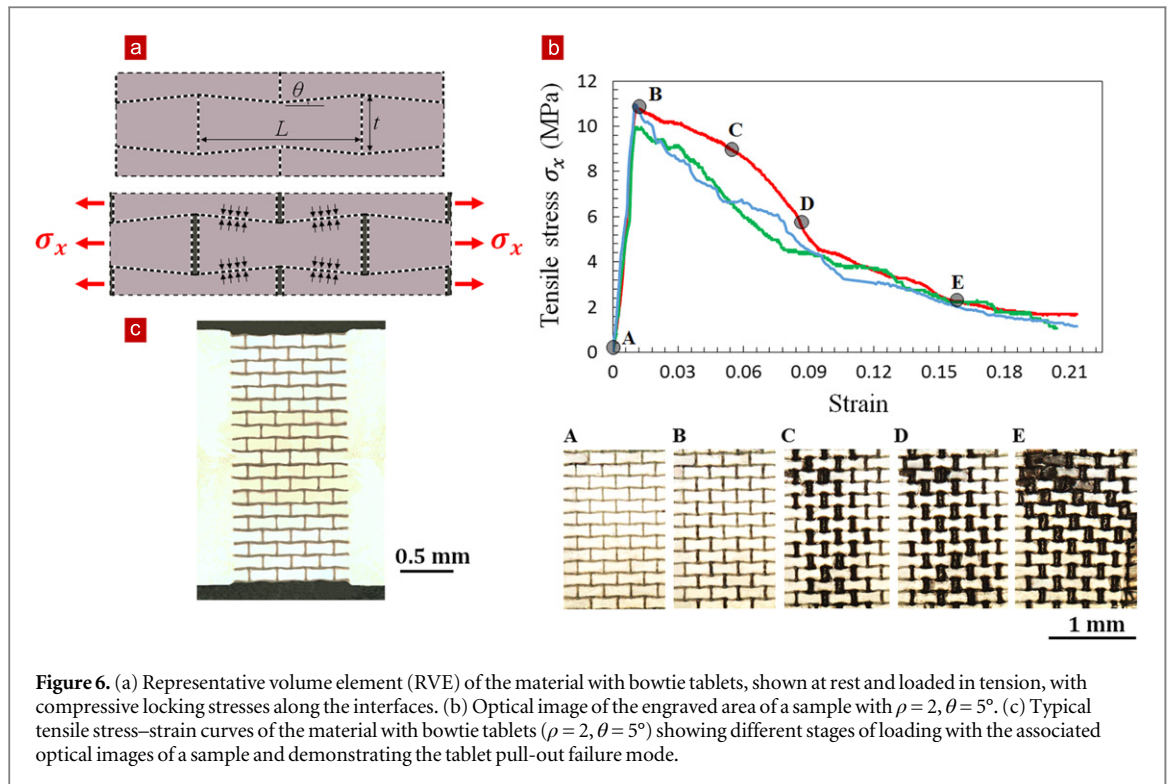
Direct observation showed that the deformation was initially uniform across the sample, which was confirmed by DIC. The initial stiffness of the nacre-like samples with $\rho = 2$ and $t = 150 \mu\text{m}$ was about 1 GPa. The tensile stress increased almost linearly until a maximum of 10 MPa (point B in figure 4(b)), which occurred at a tensile strain of about 0.01. At this point, the material entered a softening region and *in situ* imaging showed that the deformation localized along one band across the tensile direction (point C). From that point and until complete failure of the sample, all the deformation concentrated in this region while the rest of the material relaxed as the stress decreased (points D, E). Imaging revealed PU ligaments across the localization, which progressively failed as the material softened. These ligaments maintained cohesion up to average specimen tensile strains exceeding 0.2.

Our first objective was to make the tablets (i.e. the spacing between the engraved longitudinal interfaces) as thin as possible. For very thin tablets the microcracks forming the interfaces coalesced across the tablets resulting in decreased overall strength. The smallest workable distance between the longitudinal interfaces (i.e. thickness of the tablets) was $150 \mu\text{m}$, which is small compared to the nacre-like materials obtained by rapid prototyping ($t = 2 \text{ mm}$ [42]). With the thickness fixed at $t = 150 \mu\text{m}$, four aspect ratios $\rho = 1.5, 2, 3, 4$ were explored and tested in tension (figure 5(a)). The elastic modulus, strength and energy dissipation (area under the stress-strain curve)



increased by increasing the aspect ratio from 1.5 to 3, because of the increased overlap area and increased transfer of shear stress between the tablets. At low aspect ratios ($\rho \leq 2$), tablet pull-out was the dominant mode of failure. At $\rho = 3$, we observed a mixed-mode tablet pull out and tablet fracture which resulted in a large variation in the energy dissipation depending on the number of tablets which broke during the test. At higher aspect ratios ($\rho = 4$), tablet fracture was the

dominant failure mode (figure 5(c), points A–C in figure 5(a)) and as a result energy dissipation decreased significantly. The overall properties as a function of aspect ratio are shown on figure 5(b). For this system, the aspect ratio of 3 produced the best combination of strength and energy absorption, despite a few tablets fracturing upon loading of the material in tension. The transition from tablet fracture to tablet pullout is consistent with the existing models for the design of



staggered composites [39]. First, the shear strength of the interface can be estimated using [34, 39]:

$$\sigma_c = \frac{1}{2} \varphi \rho \tau_i, \quad (1)$$

where σ_c is the tensile strength of the composite, φ is the volume fraction of tablets, ρ is the aspect ratio of the tablets and τ_i is the shear strength of the interfaces. Using $\varphi = 0.93$ and the strength data of $\sigma_c \approx 10$ MPa for $\rho = 2$, the shear strength of the interface can be estimated at $\tau_i \approx 10$ MPa. The maximum aspect ratio which prevents the fracture of the tablet is, assuming a uniform shear transfer at the interfaces [39]:

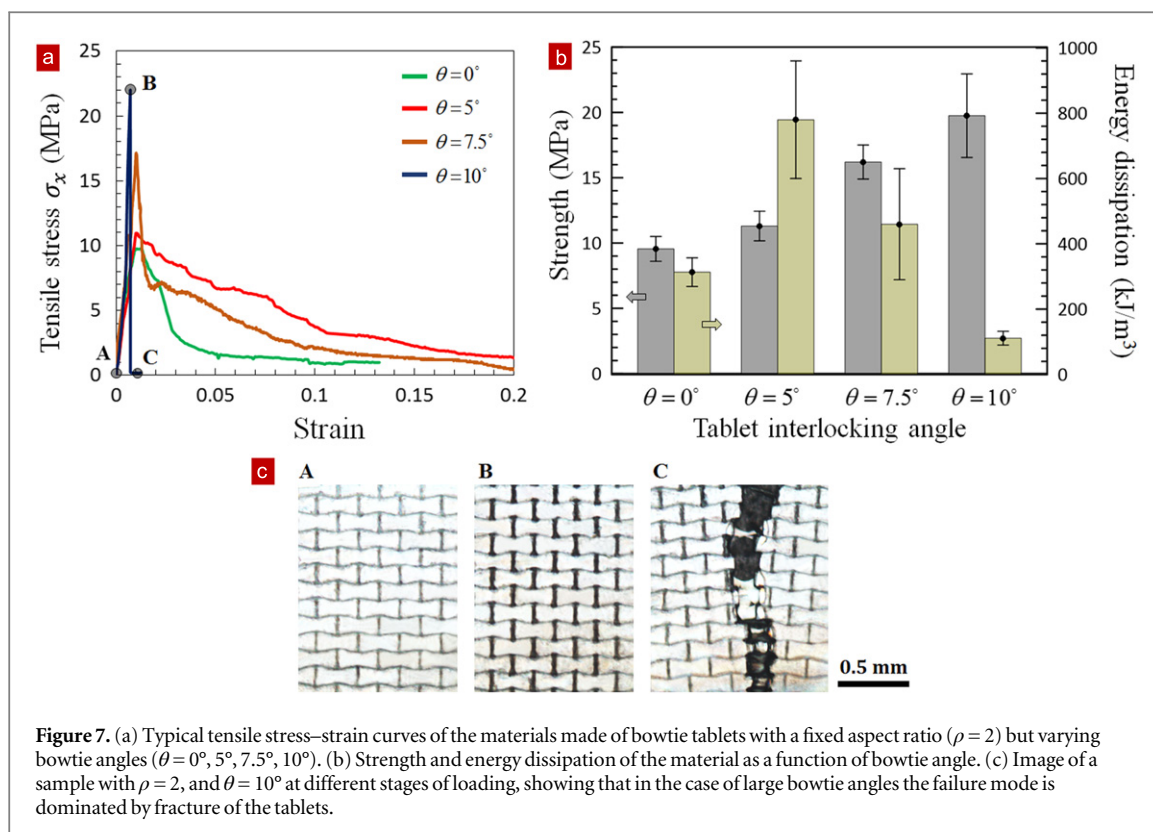
$$\rho_{\max} = \frac{1}{f_0} \frac{K_{IC}}{\tau_i \sqrt{\pi a}} - 4.7 \left[\left(\frac{a}{t} \right)^{-0.15} - 1.12 \right], \quad (2)$$

where f_0 is a geometrical factor for an edge crack in a strip of finite width, K_{IC} is the fracture toughness of the tablets, a is the size of microdefects on the surface of the tablets and t is the thickness of the tablets. Using $f_0 \approx 1.12$, $K_{IC} \approx 0.4$ MPa m^{1/2} for glass, $\tau_i \approx 10$ MPa, $a \approx 25$ μ m [19] and $t = 150$ μ m gives $\rho_{\max} \approx 3$. The experiments presented here showed a failure mode transition from tablet pulling to tablet fracture when the aspect ratio is increased from $\rho = 2$ to $\rho = 4$. The experiments and the prediction from the model therefore agree very well.

4. Inducing geometric hardening with bowtie tablets

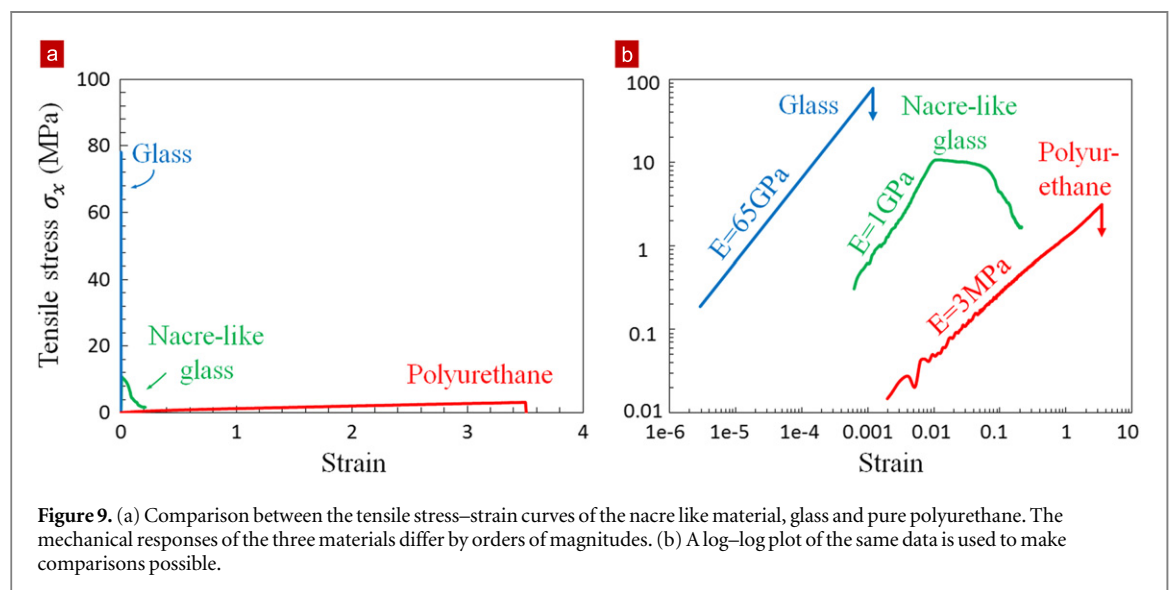
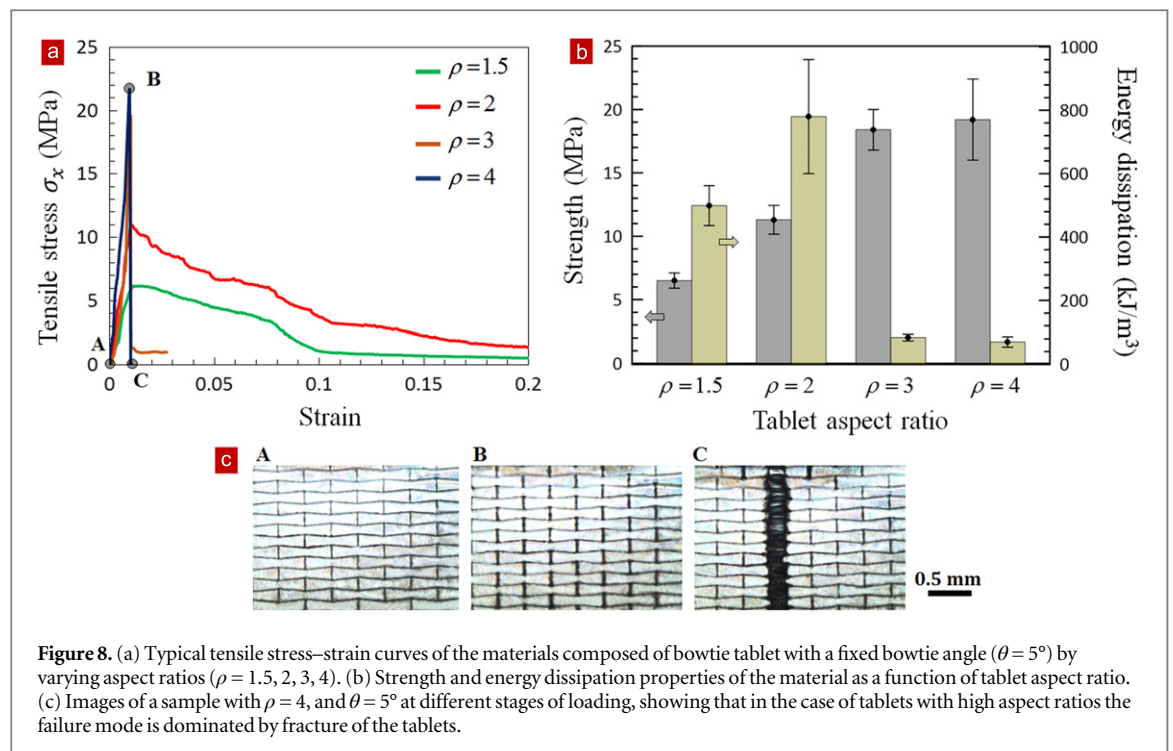
While natural proteins provide cohesion over large distances, energy absorption and the formation of ligaments in natural nacre, they are not sufficient to

produce hardening required to delay localization and spread deformations over large volumes. In natural nacre, the waviness of the tablets generates progressive locking as the tablets glide on one another (figure 1(b)). This geometrical locking largely contributes to the material resistance to deformation and prevents the localization of the strains [35]. To duplicate this geometric hardening, we fabricated another family of nacre-like materials with wavy tablets, in the form of bowties (figure 6(a)). These microstructures were characterized by the thickness t (which we fixed at $t = 150$ μ m), the aspect ratio $\rho = \frac{L}{t}$, and the bowtie angle θ . The bowtie features provided an additional resistance to pull-out by progressive locking, generating geometric hardening and delaying localization. Figure 6(b) shows the entire engraved area of a sample with bowtie tablets. The geometry of the dog-bone tensile test specimens, the number of tablets along the longitudinal and transverse directions, and the test conditions were the same as for the materials composed of flat tablets. Typical tensile stress–strain curves of the material composed of bowtie tablets with $t = 150$ μ m, $\rho = 2$, and $\theta = 5^\circ$ are shown on figure 6(c). As for flat tablets, the first portion of the stress–strain curve was quasi linear up to a maximum stress of about 10 MPa (figure 6(c), points A–B). Following the peak stress, the stress continuously decreased, but at a slow rate compared to flat tablets. *In situ* imaging of the samples (figure 6(c), points C–E) shows that in the softening region the deformations initially localized but rapidly spread over the entire sample. The material eventually failed at about 20% tensile strain, a huge amount of



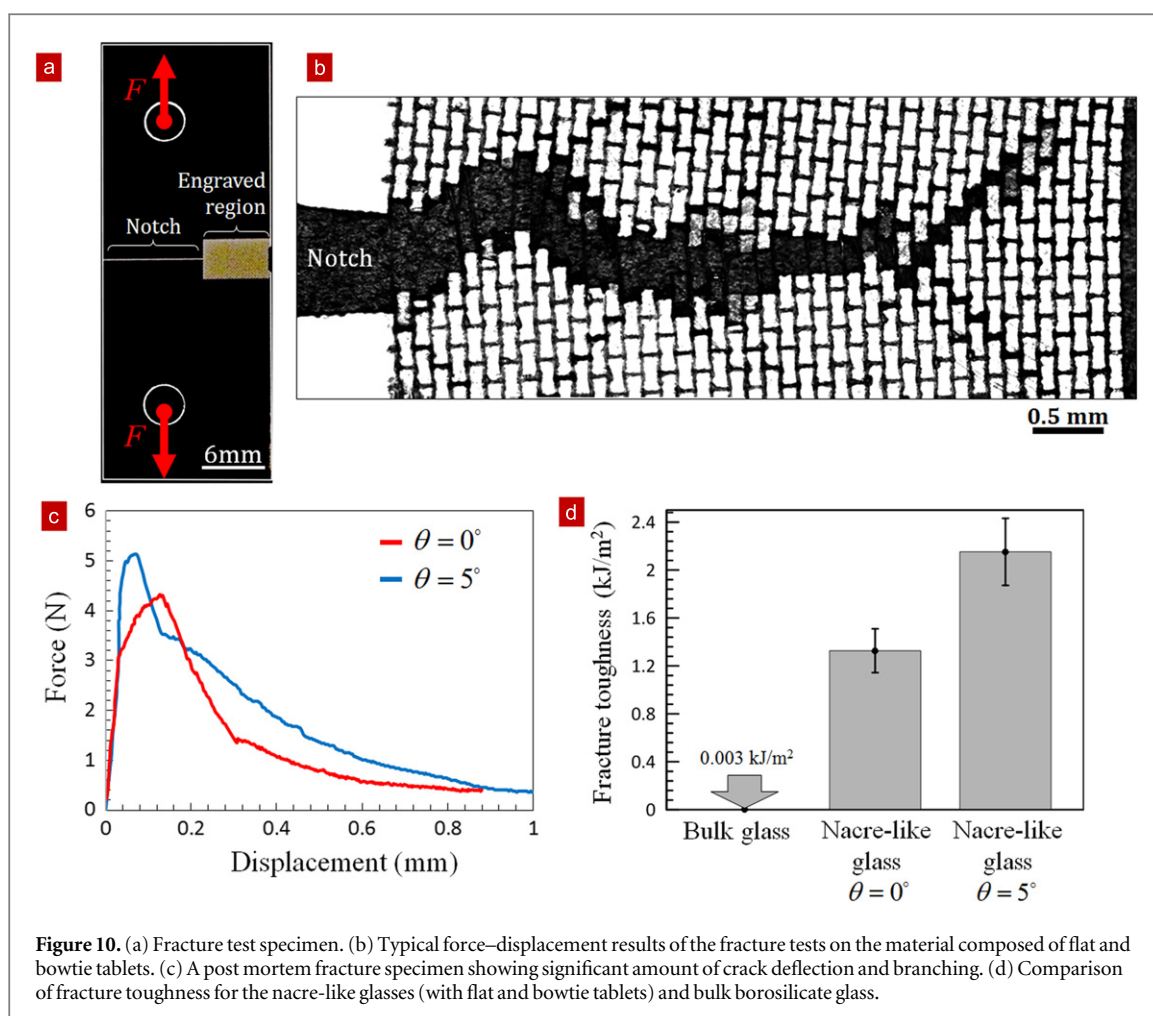
deformation for a material mostly composed of glass. Our nacre-like glass therefore duplicates the most important deformation and fracture mechanisms of nacre. Progressive tablet sliding and pull-out occurred from the combined hardening of the PU layer and the geometric hardening from the bowtie shape of the tablets. The observation of continuous spreading of the deformation despite a continuous decrease in applied stress could be an indication that strain rate hardening is operating at the interface [18], in addition to stiffening and geometric hardening. Because non-linear deformation spread over the entire material, the measured strain and energy absorption can be considered representative of large materials made with the same microstructure. For this case, the stiffness and strength of the material are ~ 1 GPa and ~ 10 MPa, and the material dissipates over 800 kJ m^{-3} of strain energy (the area under the stress–strain curve). For comparison, the stiffness, strength, and energy dissipation of the bulk glass material, obtained from four-point bending tests, are ~ 65 GPa, ~ 80 MPa, and $\sim 80 \text{ kJ m}^{-3}$ respectively. For the case of bulk glass, much of the energy however is dissipated through dynamic effects and other propagations to connective components while only a small portion is actually consumed for the formation and propagation of cracks [19, 43]. Therefore, strength and stiffness are sacrificed in our nacre-like glasses in order to obtain a significantly higher toughness. These properties can be fine-tuned by adjusting the bowtie angle and aspect ratio of the tablets.

Here, the thickness of the tablets was fixed to $t = 150 \mu\text{m}$ and materials with different combinations of bowtie angles and aspect ratios were fabricated and tested. The aspect ratio was first fixed at $\rho = 2$, and materials with different bowtie angles $\theta = 0^\circ, 5^\circ, 7.5^\circ, 10^\circ$ were explored (figure 7(a)). Bowtie angle $\theta = 0^\circ$ is identical to flat tablets, discussed in the previous section. For bowtie angles lower than 5° ($\theta \leq 5^\circ$), tablet pull-out was the dominant mode of failure whereas for higher bowtie angles ($\theta > 5^\circ$), tablet fracture was dominant (figure 7(c), points A–C in figure 7(a)) resulting in a large decrease in energy dissipation (figure 7(b)). The strength of the material however increased with bowtie angle to values ~ 20 MPa where almost all the tablets broke ($\theta = 10^\circ$). We also examined the effect of the tablet aspect ratio on the tensile behavior of the material. The bowtie angle was fixed to $\theta = 5^\circ$ and materials with different aspect ratios $\rho = 1.5, 2, 3, 4$ were fabricated and tested (figure 8(a)). For materials with tablet aspect ratios lower than 2 ($\rho \leq 2$), the tablet pullout and for higher aspect ratios ($\rho \geq 3$), the tablet failure was the dominant mode of failure (figure 8(c), point A–C in figure 8(a)). The strength and the energy dissipation of the material increased with aspect ratio till the tablets started to break ($\rho \geq 3$), resulting in a poor energy dissipation and no improvement in the strength (figure 8(b)). We found that for the set of materials and the adhesive used in this study, $t = 150 \mu\text{m}$, $\theta = 5^\circ$ and $\rho = 2$ result in an optimum microstructure when toughness is preferred over strength.



Our bio-inspired glass displayed properties which are very distinct from glass and PU. To compare these properties, we tested the pure PU in tension. Free standing PU films were prepared and cured for one week. Dog-bone samples with cross-section of $2 \times 0.4 \text{ mm}$ and gage length of 5 mm, were then cut from the film using laser cutting. The samples were then tested in tension at a displacement rate of $5 \mu\text{m s}^{-1}$. The modulus and strength of the borosilicate glass we used in this work were measured using a three-point bending configuration. Figure 9(a) shows typical tensile stress–strain curve of the nacre-like glass (tablet thickness $t = 150 \mu\text{m}$, aspect ratio $\rho = 2$, and bowtie angle $\theta = 5^\circ$), intact glass and pure PU. The contrast of mechanical behavior between

these materials is extreme, and to facilitate the comparison the stress–strain curves are re-plotted on a log–log scale on figure 9(b). The initial slope of these curves is about 1, which indicates that stress varies linearly with strain in the initial stage of deformation. The ‘height’ of these curves reflects the modulus, which is indicated on figure 9(b). In terms of modulus, strength and deformation the nacre-like glass lies between pure PU and pure glass. The nacre-like structure is 65 times softer than pure glass and 8 times weaker in strength, but it is 200 times more deformable in tension. Note that these properties are all in the in-plane direction. The surface hardness of glass is maintained in the nacre-like glass, which can be attractive in cases where surface hardness and in-plane



toughness must be combined. Compared to PU the nacre-like glass is 330 times stiffer and three times stronger. PU is however about 15 times more deformable.

5. Fracture toughness

The energy absorption capabilities of these nacre-like materials, and their ability to duplicate some of natural nacre's most important mechanisms, make them interesting candidates for toughened glasses. To further characterize these materials, we also measured their fracture toughness by engraving the patterns across a notch within 150 μm thick rectangular (15×40 mm) glass specimens. The patterns contained about 500 tablets arranged in 12 columns and 44 layers (figure 10(a)). We focused on microstructures with $t = 150$ μm and $\rho = 2$. Using these dimensions, materials with flat tablets ($\theta = 0^\circ$) and bowtie tablets ($\theta = 5^\circ$) were fabricated and tested. Figure 10(b) shows typical force–displacement curves for these materials. The curves had an overall bell shape characteristic of stable crack propagation. Following an initial linear region, crack propagated in a stable fashion: the applied force had to be increased to propagate the crack further. After a maximum at 4–5 N, the crack was less stable

and propagated faster, but following a 'gracious' failure mode in a non-catastrophic fashion and with progressive decrease in force. *In situ* imaging showed considerable crack bridging, deflection, and branching for both flat and bowtie tablets. However, the extent of crack deflection and branching was more pronounced for the material with bowtie tablets (figure 10(c)). We computed the work of fracture for each of these materials as the area under the force–displacement curve divided by the cross section area of the intact ligament ahead of the notch before fracture. Figure 10(d) shows that the nacre-like glasses were about 500–700 times tougher than bulk glass (in energy terms). Because of their more sophisticated toughening mechanisms, the materials with bowtie tablets produced higher toughness (2.15 ± 0.28 kJ m^{-2}) compared to flat tablets (1.33 ± 0.19 kJ m^{-2}). For comparison, the toughness of glass is only 3 J m^{-2} [44] (figure 10(d)). We also performed fracture toughness tests on PU interfaces using a rigid double cantilever beam configuration [19], and found toughness values of about 200 J m^{-2} . This nacre-like material therefore amplifies the toughness of both constituents: it is more than 700 tougher than borosilicate glass and more than 10 times tougher than PU. Finally, the fracture toughness K_{IC} , based on

stress intensity factor, was computed for the materials using $K_{IC} = \sqrt{J_{IC}E}$ where J_{IC} is the toughness in energy terms and E is the modulus. Using $E = 1$ GPa for the nacre-like glasses, we found $K_{IC} = 1.15$ MPa m^{1/2} for the nacre-like glass with flat tablets and $K_{IC} = 1.5$ MPa m^{1/2} for the nacre-like glass with bowtie tablets. This is 3–4 times higher than bulk glass ($K_{IC} = 0.4$ MPa m^{1/2} [45]). The nacre-like glass materials are therefore superior to glass in the context of impact resistance (high J_{IC}) but also resistance to cracking under constant force (high K_{IC}). These materials demonstrate that tremendous toughness can be achieved in synthetic materials through careful design and optimization of their microarchitecture, following the principles inspired from natural nacre.

6. Conclusion

Highly mineralized biological materials such as nacre display unusual combinations of mechanical properties such as toughness and strength, two properties which are hard to combine in engineering materials. Here, we reported the use of a laser engraving technique to fabricate nacre-like glasses which duplicate the main structural features, mechanisms and mechanical properties of natural nacre. The weak interfaces inspired from the interfaces in natural nacre were engraved within glass and infiltrated with PU. This top-down approach produces materials with a degree of microstructural fidelity which is higher than what is found in bottom up methods, and at smaller scales currently producible by 3D printing. Moreover, since the method is based on ‘fabricating’ interfaces, it suits itself perfectly to materials with very high concentration of hard material. Our nacre-like glasses show considerable amount of tablet sliding, crack bridging, crack deflection and branching which ultimately turn the brittle glass to a tough, and deformable material. The nacre-like glass is composed of 93 vol% glass, yet 700 times tougher and breaks at strains as high as 20%. The in-plane tensile strength of glass is reduced significantly, but its surface hardness is preserved. This study therefore shows that bioinspiration, through carefully selected and optimized microarchitectures, can provide pathways to toughen engineering materials. The same ideas can be implemented to overcome brittleness in other classes of materials such as ceramics whose range of applications is limited by their low toughness. Finally the method suits itself to interesting combinations and potential synergies with existing strengthening strategies such as tempering or laminating.

Acknowledgments

This work was supported by the Fonds de recherche du Québec—Nature et technologies and by the Natural Sciences and Engineering Research Council of

Canada. MM was partially supported by a McGill Engineering Doctoral Award. The authors would also like to thank Luc Mongeau and his students for access to the Digital Image Correlation software.

References

- [1] Clegg W J, Kendall K, Alford N M, Button T W and Birchall J D 1990 A simple way to make tough ceramics *Nature* **347** 455–7
- [2] Ballarini R, Kayacan R, Ulm F-J, Belytschko T and Heuer A 2005 Biological structures mitigate catastrophic fracture through various strategies *Int. J. Fract.* **135** 187–97
- [3] Yahyazadehfard M, Ivancik J, Majid H, An B, Zhang D and Arola D 2014 On the mechanics of fatigue and fracture in teeth *Appl. Mech. Rev.* **66** 030803
- [4] Kamat S, Su X, Ballarini R and Heuer A 2000 Structural basis for the fracture toughness of the shell of the conch strombus gigas *Nature* **405** 1036–40
- [5] Zimmermann E A, Gludovatz B, Schaible E, Dave N K, Yang W, Meyers M A and Ritchie R O 2013 Mechanical adaptability of the Bouligand-type structure in natural dermal armour *Nat. Commun.* **4** 2634
- [6] Gupta H S, Seto J, Wagermaier W, Zaslansky P, Boesecke P and Fratzl P 2006 Cooperative deformation of mineral and collagen in bone at the nanoscale *Proc. Natl Acad. Sci.* **103** 17741–6
- [7] Ritchie R O, Buehler M J and Hansma P 2009 Plasticity and toughness in bone *Phys. Today* **62** 41–7
- [8] Wang R Z, Suo Z, Evans A G, Yao N and Aksay I A 2001 Deformation mechanisms in nacre *J. Mater. Res.* **16** 2485–93
- [9] Barthelat F and Rabiei R 2011 Toughness amplification in natural composites *J. Mech. Phys. Solids* **59** 829–40
- [10] Smith B L, Schäffer T E, Vlani M, Thompson J B, Frederick N A, Klndt J, Belcher A, Stuckyll G D, Morse D E and Hansma P K 1999 Molecular mechanistic origin of the toughness of natural adhesives, fibres and composites *Nature* **399** 761–3
- [11] Keckes J, Burgert I, Frühmann K, Müller M, Kölln K, Hamilton M, Burghammer M, Roth S V, Stanzl-Tschegg S and Fratzl P 2003 Cell-wall recovery after irreversible deformation of wood *Nat. Mater.* **2** 810–3
- [12] Barthelat F 2007 Biomimetics for next generation materials *Phil. Trans. R. Soc. B* **365** 2907–19
- [13] Espinosa H D, Rim J E, Barthelat F and Buehler M J 2009 Merger of structure and material in nacre and bone—perspectives on de novo biomimetic materials *Prog. Mater. Sci.* **54** 1059–100
- [14] Jackson A P, Vincent J F V and Turner R M 1988 The mechanical design of nacre *Proc. R. Soc. B* **234** 415–40
- [15] Rabiei R, Bekah S and Barthelat F 2010 Failure mode transition in nacre and bone-like materials *Acta Biomater.* **6** 4081–9
- [16] Evans A G, Suo Z, Wang R Z, Aksay I A, He M Y and Hutchinson J W 2001 Model for the robust mechanical behavior of nacre *J. Mater. Res.* **16** 2475–82
- [17] Barthelat F, Tang H, Zavattieri P D, Li C M and Espinosa H D 2007 On the mechanics of mother-of-pearl: a key feature in the material hierarchical structure *J. Mech. Phys. Solids* **55** 306–37
- [18] Chintapalli R K, Breton S, Dastjerdi A K and Barthelat F 2014 Strain rate hardening: a hidden but critical mechanism for biological composites? *Acta Biomater.* **10** 5064–73
- [19] Mirkhalaf M, Dastjerdi A K and Barthelat F 2014 Overcoming the brittleness of glass through bio-inspiration and micro-architecture *Nat. Commun.* **5** 3166
- [20] Corni I, Harvey T, Wharton J, Stokes K, Walsh F and Wood R 2012 A review of experimental techniques to produce a nacre-like structure *Bioinspir. Biomimetics* **7** 031001
- [21] Tang Z, Kotov N A, Magonov S and Ozturk B 2003 Nanostructured artificial nacre *Nat. Mater.* **2** 413–8
- [22] Podsiadlo P *et al* 2007 Ultrastrong and stiff layered polymer nanocomposites *Science* **318** 80–3

- [23] Bonderer L J, Studart A R and Gauckler L J 2008 Bioinspired design and assembly of platelet reinforced polymer films *Science* **319** 1069–73
- [24] Mirkhalaf Valashani S M, Barrett C J and Barthelat F 2015 Self-assembly of microscopic tablets within polymeric thin films: a possible pathway towards new hybrid materials *RSC Adv.* **5** 4780–7
- [25] Yao H B, Tan Z H, Fang H Y and Yu S H 2010 Artificial nacre-like bionanocomposite films from the self-assembly of chitosan-montmorillonite hybrid building blocks *Angew. Chem. Int. Ed.* **49** 10127–31
- [26] Almqvist N, Thomson N H, Smith B L, Stucky G D, Morse D E and Hansma P K 1999 Methods for fabricating and characterizing a new generation of biomimetic materials *Mater. Sci. Eng. C* **7** 37–43
- [27] Walther A, Bjurhager I, Malho J M, Pere J, Ruokolainen J, Berglund L A and Ikkala O 2010 Large-area, lightweight and thick biomimetic composites with superior material properties via fast, economic, and green pathways *Nano Lett.* **10** 2742–8
- [28] Deville S, Saiz E, Nalla R K and Tomsia A P 2006 Freezing as a path to build complex composites *Science* **311** 515–8
- [29] Bouville F, Maire E, Meille S, Van de Moortèle B, Stevenson A J and Deville S 2014 Strong, tough and stiff bioinspired ceramics from brittle constituents *Nat. Mater.* **13** 508–14
- [30] Munch E, Launey M E, Alsem D H, Saiz E, Tomsia A P and Ritchie R O 2008 Tough, bio-inspired hybrid materials *Sci.* **322** 1516–20
- [31] Andres C M and Kotov N A 2010 Inkjet deposition of layer-by-layer assembled films *J. Am. Chem. Soc.* **132** 14496–502
- [32] Mirkhalaf M, Deju Z and Barthelat F 2013 *Engineered Biomimicry* ed A Lakhtakia and R J Martin-Palma (New York: Elsevier)
- [33] Kotha S P, Li Y and Guzelsu N 2001 Micromechanical model of nacre tested in tension *J. Mater. Sci.* **36** 2001–7
- [34] Begley M R, Philips N R, Compton B G, Wilbrink D V, Ritchie R O and Utz M 2012 Micromechanical models to guide the development of synthetic ‘brick and mortar’ composites *J. Mech. Phys. Solids* **60** 1545–60
- [35] Katti K S, Katti D R, Pradhan S M and Bhosle A 2005 Platelet interlocks are the key to toughness and strength in nacre *J. Mater. Res.* **20** 1097–100
- [36] Gao H, Ji B, Jäger I L, Arzt E and Fratzl P 2003 Materials become insensitive to flaws at nanoscale: lessons from nature *Proc. Natl Acad. Sci.* **100** 5597–600
- [37] Bekah S, Rabiei R and Barthelat F 2011 Structure, scaling, and performance of natural micro- and nanocomposites *BioNanoScience* **1** 1–9
- [38] Askarinejad S and Rahbar N 2015 Toughening mechanisms in bioinspired multilayered materials *J. R. Soc. Interface* **12** 20140855
- [39] Barthelat F 2014 Designing nacre-like materials for simultaneous stiffness, strength and toughness: optimum materials, composition, microstructure and size *J. Mech. Phys. Solids* **73** 22–37
- [40] Dimas L S, Bratzel G H, Eylon I and Buehler M J 2013 Tough composites inspired by mineralized natural materials: computation, 3D printing, and testing *Adv. Funct. Mater.* **23** 4629–38
- [41] Barthelat F and Zhu D 2011 A novel biomimetic material duplicating the structure and mechanics of natural nacre *J. Mater. Res.* **26** 1203–15
- [42] Lin E, Li Y, Ortiz C and Boyce M C 2014 3D printed, bio-inspired prototypes and analytical models for structured suture interfaces with geometrically-tuned deformation and failure behavior *J. Mech. Phys. Solids* **73** 166–82
- [43] Barinov S 1993 Work-of-fracture determination for brittle materials *J. Mater. Sci. Lett.* **12** 674–6
- [44] Lawn B 1993 *Fracture of Brittle Solids* (Cambridge: Cambridge University Press)
- [45] Wiederhorn S and Bolz L 1970 Stress corrosion and static fatigue of glass *J. Am. Ceram. Soc.* **53** 543–8